Technical note: Measurement of chemically-resolved volume equivalent diameter and effective density of particles by AAC-SPAMS

Long Peng[1,2], Lei Li[4], Guohua Zhang[1, 3*], Xubing Du[4], Xinming Wang[1, 3], Ping'an Peng[1, 3], Guoying Sheng[1], Xinhui Bi[1, 3*]

[1] State Key Laboratory of Organic Geochemistry and Guangdong Provincial Key Laboratory of Environmental Protection and Resources Utilization, Guangzhou Institute of Geochemistry, Chinese Academy of Sciences, Guangzhou 510640, China

[2] University of Chinese Academy of Sciences, Beijing, 100049, China

[3] Guangdong-Hong Kong-Macao Joint Laboratory for Environmental Pollution and Control, Guangzhou 510640, China

[4] Institute of Mass Spectrometer and Atmospheric Environment, Jinan University, Guangzhou 510632, China

*Correspondence to: bixh@gig.ac.cn and zhanggh@gig.ac.cn

This supporting information contains 8 pages, including four figures and one table

Table S1. Sampling schedule for atmospheric particles by AAC-SPAMS

Sampling duration	D_a
07/06 14:45-15:28	
07/06 22:51-23:48	
07/07 09:16-09:58	
07/07 13:39-14:20	
07/07 18:15-18:58	250.0 nm, 350.0 nm, 450.0 nm, and 550.0 nm
07/07 22:35-23:18	
07/08 06:43-07:26	
07/08 09:18-10:12	
07/08 15:19-16:04	

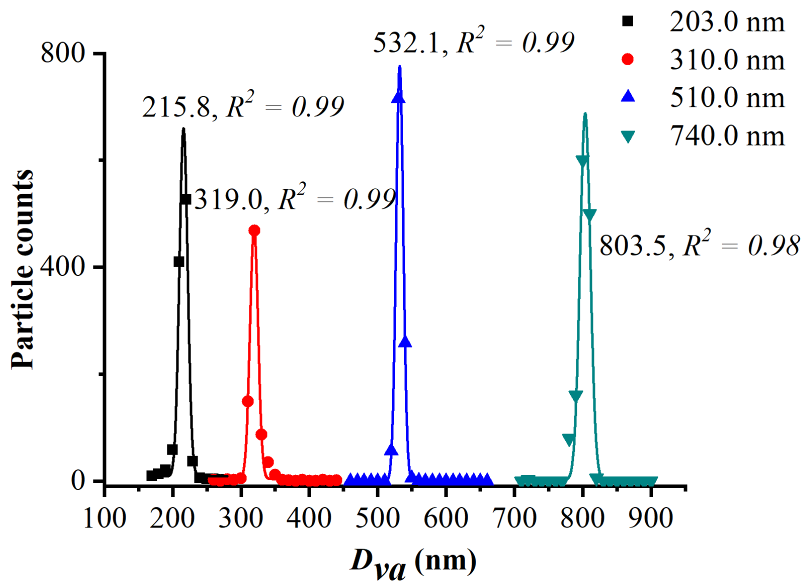

Figure S1. Gaussian fitting for the D_{va} size distribution of an aerosol of spherical PSL particles with D_{ve} values of 203.0 nm, 310.0 nm, 510.0 nm, and 740.0 nm after screening by the AAC.

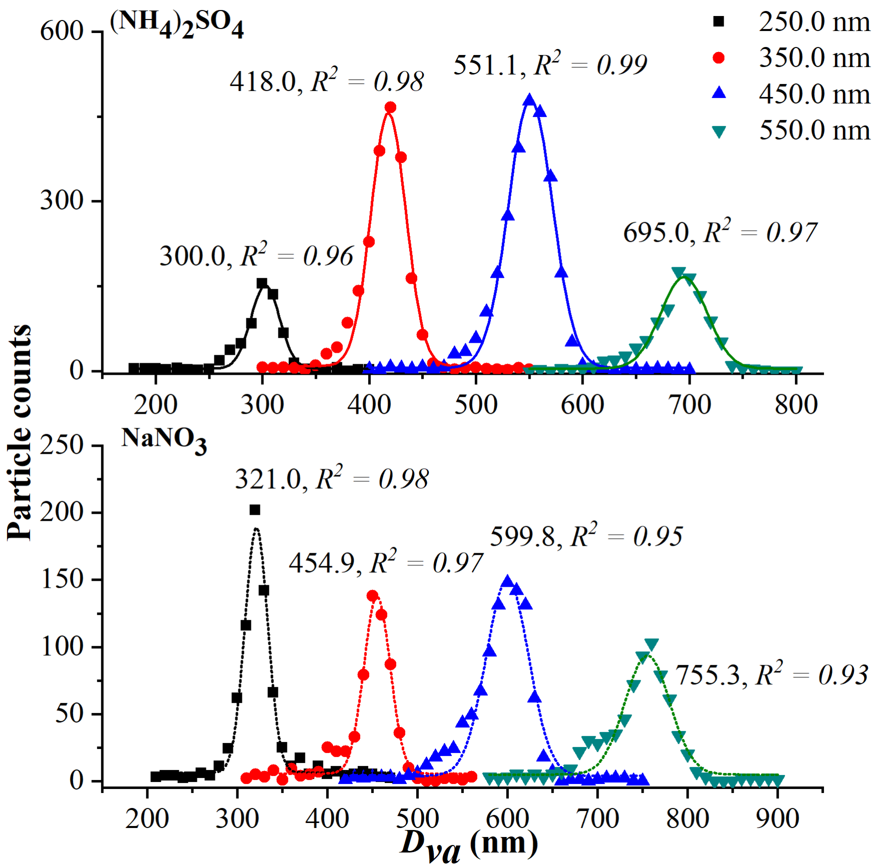

Figure S2. (a) Gaussian fitting for the D_{va} size distribution of the aspherical aerosol particles of $(NH_4)_2SO_4$ and $NaNO_3$ with D_a values of 250.0 nm, 350.0 nm, 450.0 nm, and 550.0 nm. (b) Comparison between the χ_t and the measured χ_v of the $(NH_4)_2SO_4$ and $NaNO_3$ particles.

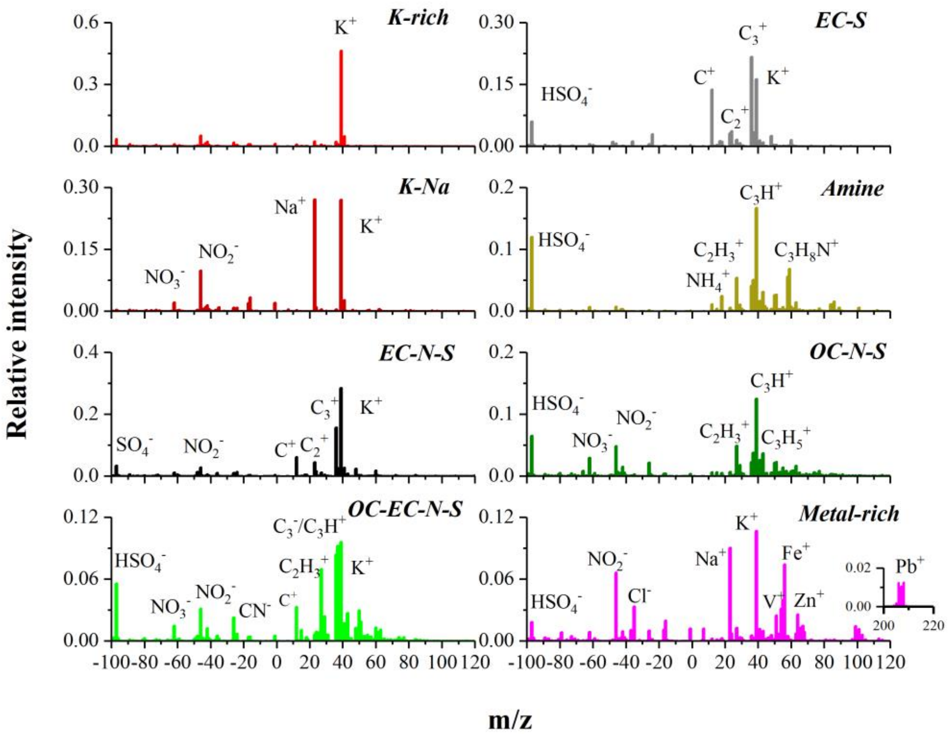

Figure S3. Average positive and negative mass spectra for eight major types

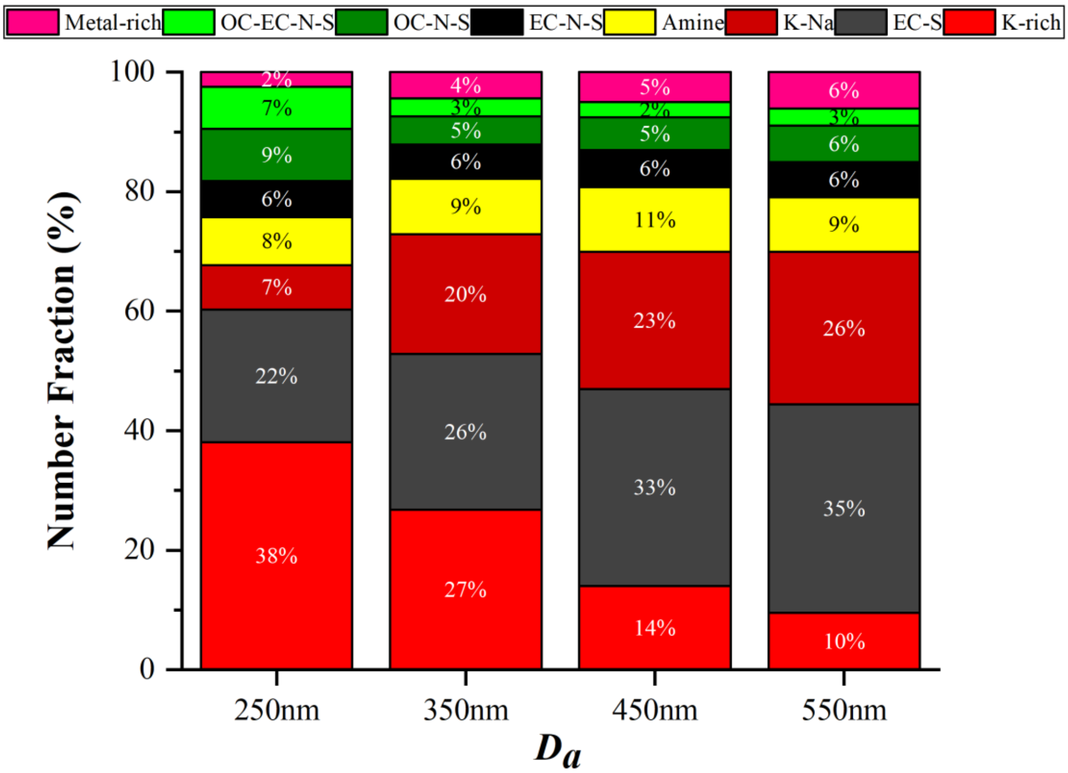

Figure S4. Aerodynamic diameter-resolved chemical composition of different type particles.

Figures S3 and S4 show the average positive and negative digitized mass spectra of eight types particles and their number fraction distribution from 250 nm to 550 nm, respectively. The K-rich spectra are characterized by the dominant potassium ($39[K]^+$), which number fraction decreases from 38% at 250 nm D_a to 10% at 550 nm D_a. Elemental carbon ($12[C]^+$, $24[C_2]^+$ and $36[C_3]^+$) and sulfate ($-97\ [HSO_4]^-$) are the dominant peaks in EC-S which number fraction increases from 22% at 250 nm to 35% at 550 nm. K-Na particles possess the distinct sodium ($23[Na]^+$) and potassium in positive spectra and nitrate ($-46\ [NO_2]^-$ and/or $-62\ [NO_3]^-$) in the negative spectra, comprising 7% number fraction at 250 nm and 26% at 550 nm. Amine particles distinguish them from other particles by organic amine fragments such as $58[C_3H_8N]^+$, accounting for about 9% for particles with D_a from 250 nm to 550 nm. The types of EC-N-S, OC-N-S and OC-EC-N-S have similar predominant peaks of sulfate and nitrate in the negative spectra. The makers of carbonaceous matters differentiate EC-N-S, OC-N-S and OC-EC-N-S. The spectra of EC-N-S mainly contains elemental carbon, and the spectra of OC-N-S mainly possesses hydrocarbon ion series such as $27[C_2H_3]^+$ and $37[C_3H]^+$, and the spectra of OC-EC-N-S has markers of both of elemental carbon and organic carbon. The proportions of types of EC-N-S, OC-N-S and OC-EC-N-S in the whole size range are relatively stable with 6%, 7%, and 3%, respectively. The Metal-rich particles are dominated by peaks at $51[V]^+$, $54/56[Fe]^+$, $64/66/68\ [Zn]^+$ and $206/207/208\ [Pb]^+$, which number fraction increase from 2% at 250 nm to 6% at 550 nm.